

PREDICTION OF THE EXCITATION FORCE OF AN AIR COMPRESSOR AT THE MOUNTING POSITION BY VIBRATION TRANSFER PATH ANALYSIS

KWANJU KIM¹, UYUP PARK¹, SEUNG-GON KIM² & MIN-GYEONG KIM²

¹Hongik University, Korea

²Korea Railroad Research Institute of Science and Technology, Korea

ABSTRACT

Urban rapid transits are one of the most popular transportation methods these days. They are equipped with large-capacity air compressors because they use pneumatic pressure to supply power for braking, door opening and closing. Passengers tend to complain about vibration and noise generated during the operation of the air compressor. To address such issues, the excitation force generated in an air compressor mounted on a railway car was indirectly measured in this study. In order to accurately predict the excitation force transmitted to the mount rubber, the impedance matrix method technique was applied, which uses acceleration and the inverse of transfer functions. The proper locations of the measuring acceleration were also investigated. The calculated results of the transmitting force were then compared with the directly measured values.

Keywords: air compressor; frequency response function, impedance matrix method, transfer path analysis, vibration.

1 INTRODUCTION

Railway vehicles are equipped with large-capacity air compressors because they use pneumatic pressure to supply power for braking, door opening and closing. Complaints from passengers are often raised against annoying vibration and noise generated during the operation of the air compressor. To solve such issues, it is necessary to either reduce the unbalance force occurred by the compressor or to minimize the transfer force of the air compressor excitation to the vehicle frame. In this study, the transferring system from the air compressor to the railway frame is especially concerned. An indirect method of measuring the force transferred from the air compressor is performed to predict the force acting on the mounting rubber and to investigate the proper locations of the measuring acceleration. The acceleration values in the air compressor in the operating state and the transfer functions in the stopped state are measured using an impact hammer and an accelerometer. Using the measured transfer functions and the acceleration values, the transfer force is then predicted by the impedance matrix method and is then compared with the directly measured force values [1].

This article is organized as follows. The first section shows the contribution of the air compressor's excitation to the overall vibration and the acoustic amount inside the railway cabin when a railway vehicle is running; the next section introduces the impedance matrix method used to predict the transferring forces and the three cases of different location of accelerometer. Force excitation has been carried out to predict the transferring force accurately. Finally, in the last section, the actual experiments conducted to verify the impedance matrix method by comparing the estimated force with the measured force will be explained.

2 NVH EXPERIMENT INSIDE RAILWAY VEHICLE CABIN

2.1 Setup of NVH experiment on railway vehicle interior

The vibration and noise measurements on the cabin floor above the air compressor on the operating railroad vehicle have been carried out. The NVH contribution of an air compressor on the railway vehicle has been investigated.

The four acceleration points on the floor and the two sound pressure points located 1.5 m above the floor were measured. A photograph of the experiment scene is shown in Fig. 1 and the configuration of the equipment used is shown in Fig. 2.

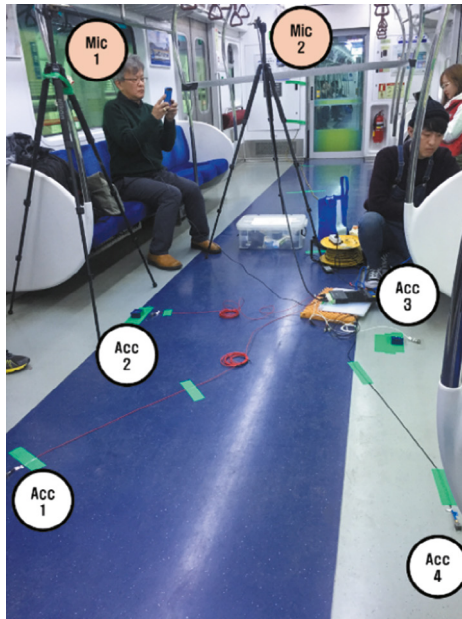


Figure 1: Vibration and noise experiments carried out in the running railway vehicles. Four accelerations and two sound pressures were measured.

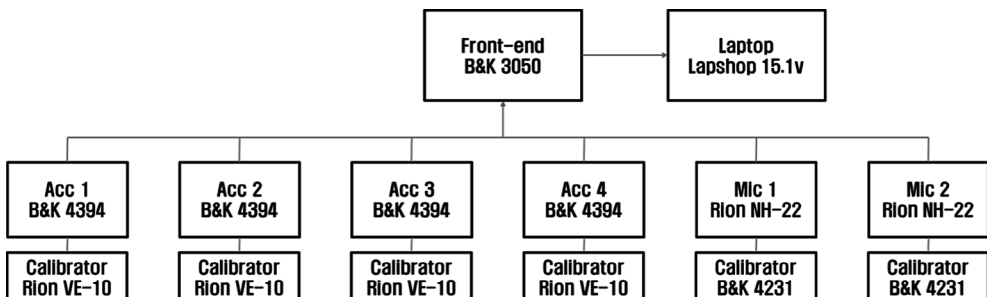


Figure 2: Configuration diagram of equipment used for NVH measurement.

2.2 Results of NVH experiment on railway vehicle interior

Figure 3 shows the time–vehicle speed (bold line) and time–acceleration magnitude for an exemplary location. Zero running speed means that the vehicle stopped at the station. In this figure, it is difficult to find out the influence of the air compressor on the vibration and noise and the operating period of the air compressor.

The acceleration information is transformed into frequency domain every 2 s using fast fourier transform (FFT) routine in MATLAB [2]. The maximum frequency was 200 Hz, and the frequency line interval was 0.5 Hz. The result is shown in Fig. 4. A typical NVH phenomena in railway vehicles clearly occurred. The first group is the vibration below 20 Hz caused by wheel–rail interface, such as rolling noise. The second group is the vibration that occurred in proportion to the vehicle speed shown between 300 and 400 s. The cause of this vibration is due to the unbalance in the rotating components such as wheel. The last group is the vibration shown from 240 to 300 s at 29.5 and 176 Hz, indicated by the downward arrows. 29.5 Hz corresponds to the rotational speed of the compressor crankshaft at 1,750 rpm. 176 Hz is sixth order of the fundamental frequency, which is 29.5 Hz in value. This vibration is caused by the shape of the rotor of the motor and/or the pulse from the electronic components. As it can be seen from these figures, in order to investigate the vibration of the air compressor clearly, NVH tests should be carried out when the railway vehicle stops at the station. Figure 5 shows the acceleration magnitude at the location of accelerometer 1 in the frequency domain depending on the air compressor operation. The magnitude of the acceleration during the compressor operation is 80 times larger than when the compressor stopped operating at 176 Hz.

3 PREDICTION OF TRANSMITTING FORCES FROM AIR COMPRESSOR ON TEST JIG USING IMPEDANCE MATRIX METHOD

When the air compressor is on, the vibration magnitude on the floor of the railroad car exhibits approximately two digits larger value than the vibration level when the air compressor is turned off. To reduce this vibration efficiently, a systematic design procedure of the mounting

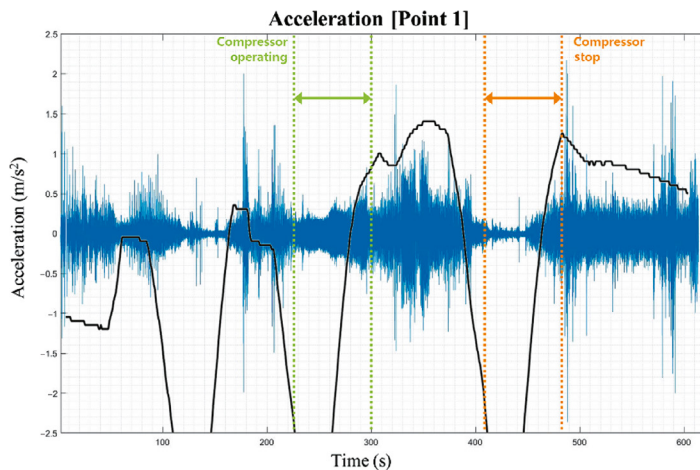


Figure 3: Time vs. railway car running speed (bold solid line) and time vs. acceleration magnitude at accelerometer 1. Air compressor operating and stopping periods are shown by dotted lines.

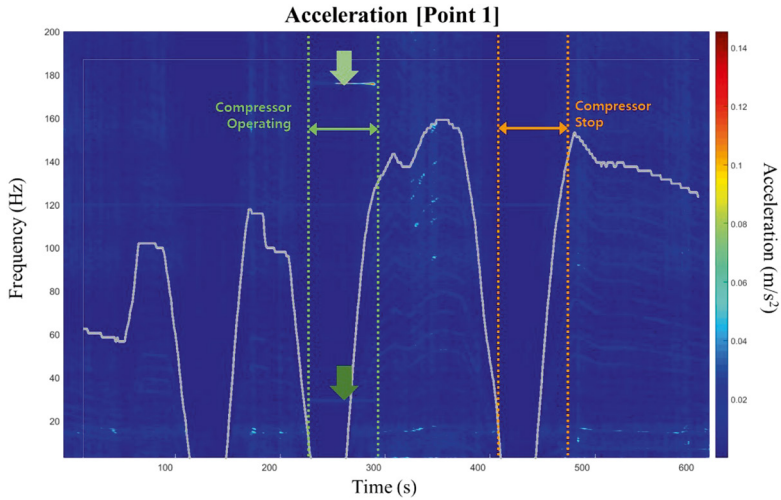


Figure 4: Time vs. railway running speed (bold solid line) and frequency vs. acceleration magnitude at accelerometer 1 for every 2 s. Air compressor operating period is shown by down arrows at 29.5 and 176 Hz

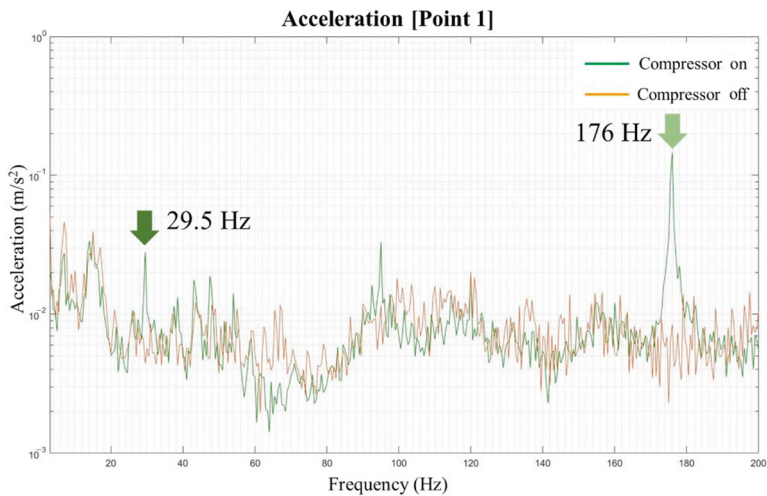


Figure 5: The acceleration magnitude at location of accelerometer 1 in the frequency domain depending on air compressor operation (green line: the air compressor on, orange line: the air compressor off).

rubber between a car body and the air compressor should be ensured. One of the necessary information for designing the mounting rubber is the exact force characteristics acting on the mount rubber. It is difficult to measure the transmitted force directly in the actual railway vehicles. Instead, an indirect measurement scheme for estimating transmitted force to each mounting rubber by using the measured values of acceleration and the transfer function

are often used. In this study, the transfer forces were estimated using the impedance matrix method. The predicted transmitted forces were then compared with those measured directly on test jig. To accurately predict the transmitted forces, adequate positions of accelerometers and impact hammer excitations were investigated.

3.1 Research flow chart using the impedance matrix method

The impedance matrix method was used among the transfer path analysis (TPA) techniques that can recover the input signal using the frequency response function (FRF) and the response signal. The relationship between the input signal, the FRF and the response signal is shown in the following eqn (1).

$$\{V\} = [H_{FV}]\{F\} \tag{1}$$

where $\{V\}$ is the acceleration measured at the accelerometer position, $[H_{FV}]$ is the FRF matrix measured between the exciter and the accelerometer and $\{F\}$ is the excitation force measured at the excitation point. Multiplication of $[H_{FV}]^{-1}$ on both sides of eqn (1) yields eqn (2) that can be used to derive the input force of $\{F\}$.

$$\{F\} = [H_{FV}]^{-1}\{V\} \tag{2}$$

Figure 6 shows the flow chart of this study. The first step is to derive the FRF at each mounting position of the air compressor when it is turned off. In the second step, the air compressor should operate and acceleration at each mounting position is to be measured. In the third step, $\{F_{cal}\}$ is calculated using the impedance matrix method. In the fourth step, the transferring force $\{F_{op}\}$ at every mounting position of the operating air compressor is directly measured. The final step is to compare and verify the results of Steps 3 and 4. When this method is verified, the force acting on the mounting rubber can be predicted accurately and can also be used for designing the mounting rubber.

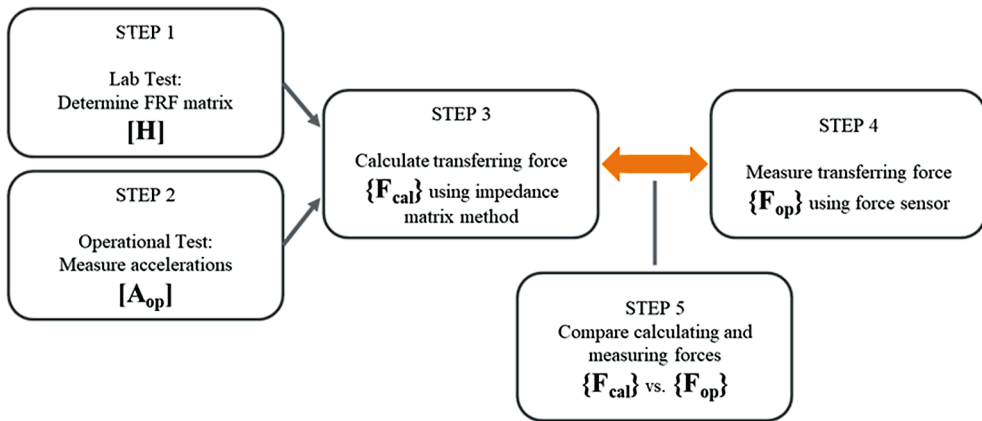
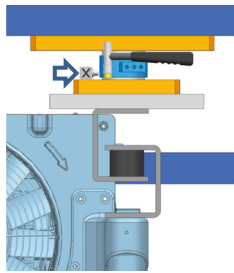
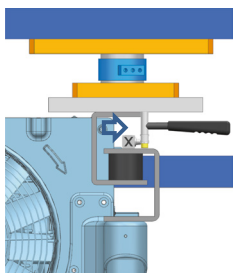
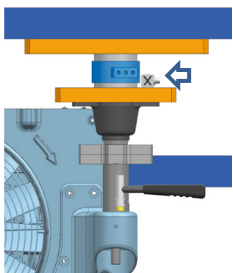


Figure 6: Research flow chart for calculating excitation force and comparing it with directly measured force.

Table 1: Three cases of positions of the accelerometer and force excitation.

	Case 1	Case 2	Case 3
CAD model			
Accelerometer position	Passive (frame) side	Active (compressor) side	Passive (frame) side
Force excitation position	Passive (frame) side	Active (compressor) side	Active (compressor) side

3.2 Locations of the accelerometers

It is known that the accelerometer is usually located in the passive(frame) side to measure FRF in TPA method [3, 4]. However, since the force generated in the air compressor is attenuatively passing the mounting rubber, it is difficult to derive the FRF exactly. Therefore, in order to predict the response function accurately, three cases of experiments have been carried out depending on the position of the accelerometer and the force excitation. The contents of the three cases are shown in Table 1.

4 COMPARISON OF THE RESULTS

The specifications of the air compressor tested in this study were two cylinders and 1,000 L/min. Operational speed was 1,450 rpm, and the pressure inside the air tank was kept constant at 9 bar. The tested air compressor is shown in Fig. 7.

4.1 Laboratory test: determining FRF matrix $[H_{FV}]$

The air compressor is mounted on the frame at four points. The transfer function $[H_{FV}]$ is obtained at the four mounting rubber positions and the size of the transfer function matrix is 4×4 . The considered frequency range was 0–200 Hz and the frequency line was 0.5 Hz. $[H_{FV}]_{21}$ and $[H_{FV}]_{12}$ in Case 3 are shown in Fig. 8, which shows the well-matched reciprocity.

4.2 Operational test: measuring acceleration $[A_{op}]$

The acceleration at each mounting was measured when the air compressor is operating. The results of the acceleration measurement are shown in Fig. 9. Acceleration values at four different points show peak values at the same frequencies. 24.5 Hz is the driving frequency of

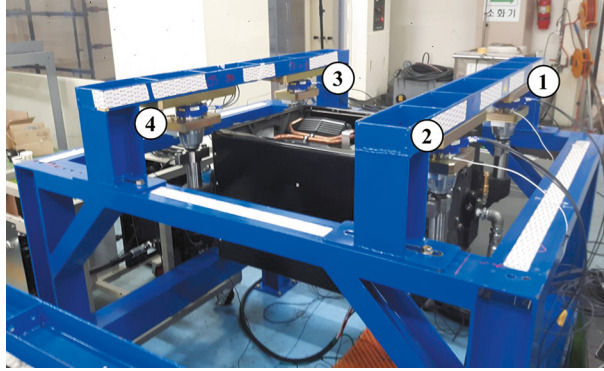


Figure 7: The tested air compressor which is mounted at four points on the frame.

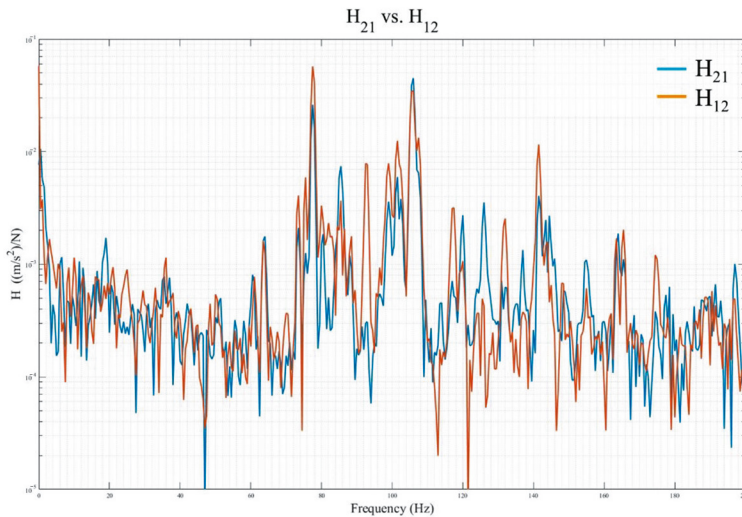


Figure 8: Measured FRF $[H_{FV}]_{21}$ and $[H_{FV}]_{12}$ in Case 3 ($[H_{FV}]_{ij}$: accelerometer position, j : force excitation position).

the air compressor and 48 Hz is the second harmonic component, while 73 Hz is the third harmonic component. To investigate the cause of the peak values at 73 and 122 Hz, frame finite-element analysis was performed with NX Nastran Simulation. 73 Hz is the first bending mode and 122 Hz is the second bending mode of the frame.

4.3 Comparison of the calculated transferring force $\{F_{cal}\}$ with the measured transferring force $\{F_{op}\}$

The calculated transferring force $\{F_{cal}\}$ at point 1 using eqn (2) and the measured transferring force $\{F_{op}\}$ at the identical point 1 are shown in Fig. 10 for Cases 1 and 2, and Case 3 is shown in Fig. 11.

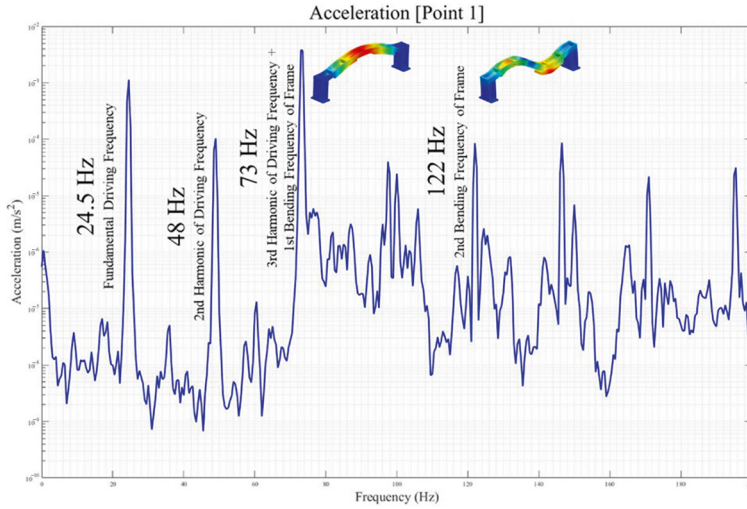


Figure 9: Measured acceleration $[A_{op}]$ at point 1 in Case 3.

In all cases, the peak frequencies of the predicted transferring force were estimated accurately. However, the magnitude of the predicted transferring force at the driving frequency is similar to that of the actual transferring force in Case 1 (passive side). It differs from the actual transferring force in the harmonic components. In Case 2 (active side), predicted force

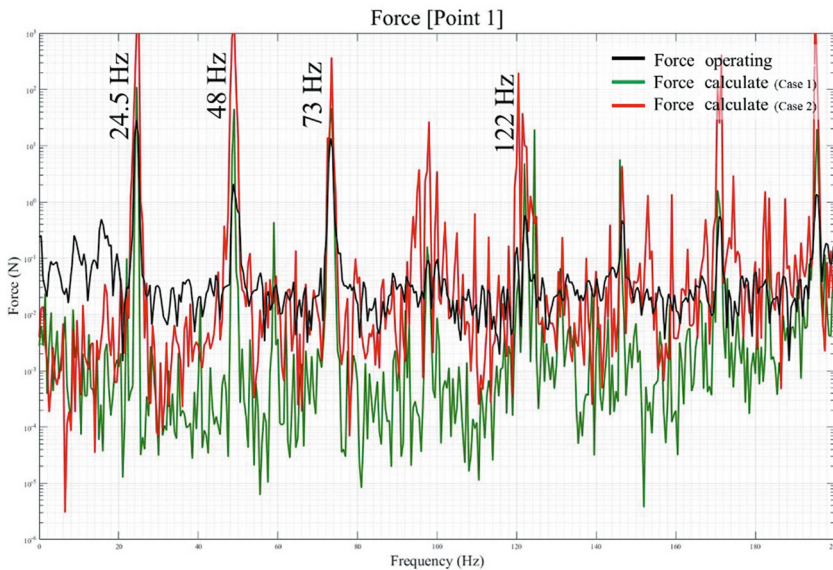


Figure 10: Comparing transferring force $[F_{cal}]$ with $[F_{op}]$ in Case 1 and Case 2 at point 1 (green line: calculated transferring force in Case 1, red line: calculated transferring force in Case 2, black line: measured transferring force with force sensor).

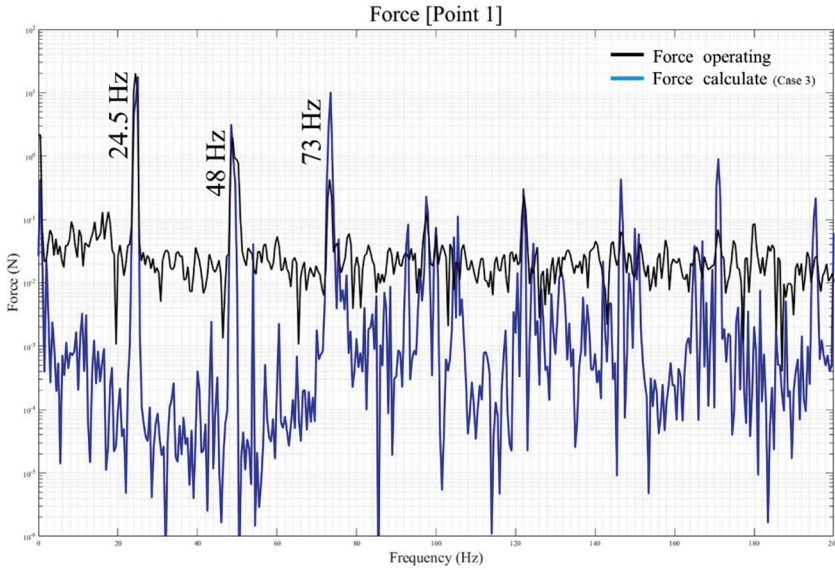


Figure 11: Comparing transferring force $[F_{cal}]$ with $[F_{op}]$ in Case 3 at point 1 (blue line: calculated transferring force in Case3, black line: measured transferring force with force sensor).

is 1 or 2 digits larger than the actual force. The reasons are as follows: the location of accelerometer in the compressor side and the robustness of the transfer function $[H_{FV}]$. In Case 3, the peak values agree well at 24.5 and 48 Hz. At 73 Hz which is the third harmonic of driving frequency, the peak values do not match because of the first bending mode of the frame jig. Therefore, Case 3 is thought to be the most appropriate method to predict the transferring force.

5 CONCLUSION

In this study, the impedance matrix method, the indirect method of measuring the excitation force generated in an air compressor mounted on a railway car, was performed and the proper locations of the measuring acceleration were investigated.

The contribution of the air compressor vibration was clearly identified when the railway vehicle stopped at the station.

As far as the location of the accelerometer and force excitation are concerned, all three cases showed that the predicted peak frequencies of transferring force match well with those of measurement results. Especially in Case 3, the peak values agreed well both at the fundamental frequency and at second harmonics. Therefore, it is recommended to place accelerometers at the passive side and the force excitation at the active side.

ACKNOWLEDGEMENTS

This research was supported by 2016 Hongik University Research Fund and a grant (17RTRP-B122846-03) from Railroad Technology Research Program funded by Ministry of Land, Infrastructure and Transport of Korean Government.

REFERENCES

- [1] Lyon, R., *Machinery Noise and Diagnostics*, Butterworths: Oxford, pp. 189–220, 1987.
- [2] Randall, R.B., *Frequency Analysis*, Larsen & Son A/S: Glostrup, pp. 271–304, 1987.
- [3] Tcherniak, D., Application of transmissibility matrix method to structure borne path contribution analysis. *Proceedings of NAG/DAGA-2009 Conference*, Rotterdam, Netherlands, 2009.
- [4] Noumura, K. & Yoshida, J., Method of transfer path analysis for vehicle interior sound with no excitation experiment, F2006D183. *Proceedings of FISITA World Automotive Congress*, Yokohama, Japan, 2006.